Journal of Sound and Vibration (2001) **245**(2), 375–383
doi:10.1006/jsvi.2000.3539, available online at http://www.idealibrary.com on IDEAL®

A HYSTERESIS MODEL FOR THE FIELD-DEPENDENT DAMPING FORCE OF A MAGNETORHEOLOGICAL DAMPER

S.-B. Choi and S.-K. Lee

Smart Structures and Systems Laboratory, Department of Mechanical Engineering, Inha University, Incheon 402-751, *Korea. E-mail: seungbok@inha.ac.kr*

AND

Y.-P. Park

Department of Mechanical Engineering, Yonsei University, Seoul 120-749, *Korea*

(*Received* 18 *September, and in final form* 7 *December* 2000)

1. INTRODUCTION

Recently, many types of semi-active electrorheological (ER) or magnetorheological (MR) dampers have been proposed for vibration attenuation of various dynamic systems including vehicle suspensions. It has been demonstrated via experimental realization that unwanted vibrations of application systems can be effectively controlled by employing ER or MR dampers associated with appropriate control strategies [1, 2]. One of the very important factors to successfully achieve desirable control performance is to have an accurate damping force model which can capture the inherent hysteresis behavior of ER or MR dampers. Especially, a more accurate damper model is required in the realization of an open-loop control which is easy to implement and cost-effective comparing with a closed-loop control. So far, several damper models have been proposed to predict the field-dependent hysteresis behavior of ER or MR dampers. These include Bouc–Wen model [3], non-linear hysteretic biviscous model [4], and a modified Bingham plastic model [5]. The validity of these models for predicting the hysteresis behavior has been favorably proved by comparing with experimental results. However, using these models, it is very difficult to realize a control system (open-loop or closed-loop) to achieve desirable tracking control performance of the field-dependent damping force. This is because the experimental parameters used in the models are basically varied with respect to the intensity of the applied field.

Consequently, the main contribution of this work is to propose a hysteresis damper model which can be easily integrated with a control system. In order to achieve the goal, a cylindrical type of MR damper, which can be applicable to a middle-sized passenger vehicle, is adopted and its hysteresis behavior is experimentally evaluated in the damping force versus piston velocity domain. The measured hysteresis characteristics of the field-dependent damping forces are compared with those predicted from the models; simple Bingham model, Bouc-Wen model and the proposed polynomial model. In addition, the accuracy of the damping force control using the proposed model is experimentally demonstrated through the open-loop control scheme. It is remarked that of the research published, none deals with the investigation of the damping force tracking control by utilizing the hysteresis models.

2. DAMPING FORCE MODELS

The schematic configuration of an automotive MR damper adopted in this work is shown in Figure 1. The MR damper is divided into the upper and lower chambers by the

0022-460X/01/320375 + 09 $35.00/0

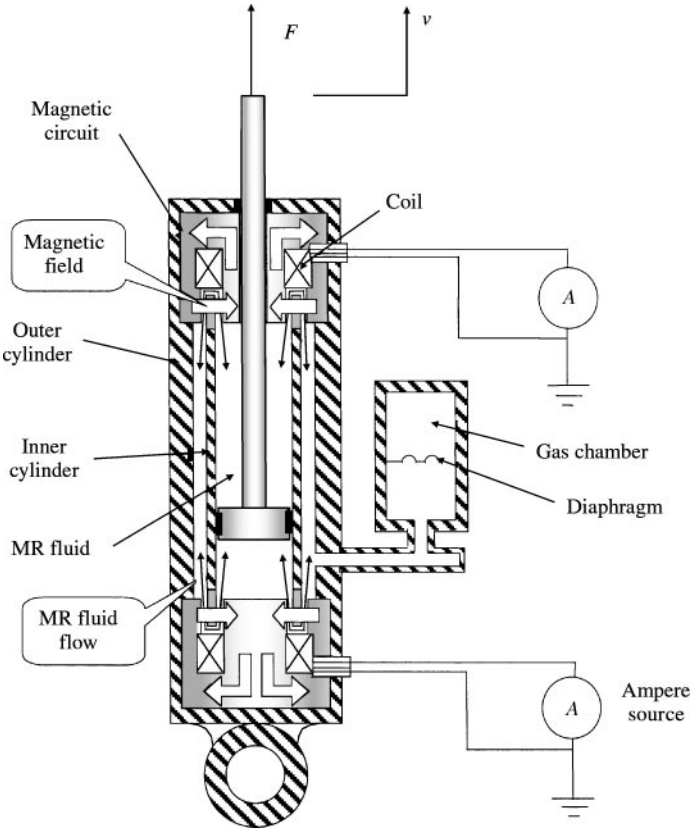

Figure 1. Configuration of the MR damper.

piston, and it is fully filled with the MR fluid; Lord product MRF132-LD. The principal design parameters are chosen as follows—the outer radius of the inner cylinder: 30·1 mm, the length of the magnetic pole: 10 mm, the gap between the magnetic poles: 1·0 mm, the number of coil turns: 150, and the diameter of the copper coil: 0·8 mm. The gas chamber is fully charged by nitrogen and its initial pressure at the maximum extension (up motion of the piston) is set as 25 bar. Figure 2 presents the measured damping force versus piston velocity at various input currents (magnetic fields). The result is obtained by exciting the MR damper with the excitation frequency of 1·4 Hz and the exciting magnitude of ± 20 mm. The details for the measurement procedures are well described in reference [6]. It is clearly observed from Figure 2 that the magnitude of the damping force at a certain piston velocity increases as the input current increases. Moreover, it is seen that the hysteresis loop is also increased with the increment of the input current.

In this work, we consider three different damper models to predict the field-dependent damping force characteristics shown in Figure 2. The first model is a simple Bingham model and its basic mechanism is represented by Figure 3(a). In Bingham model, the yield stress (τ_y) of the MR fluid is expressed by

$$\tau_y = \alpha H^{\beta}, \tag{1}$$

where H is the magnetic field, α and β are intrinsic values of the employed MR fluid which are to be experimentally identified. Thus, the damping force of the MR damper can be

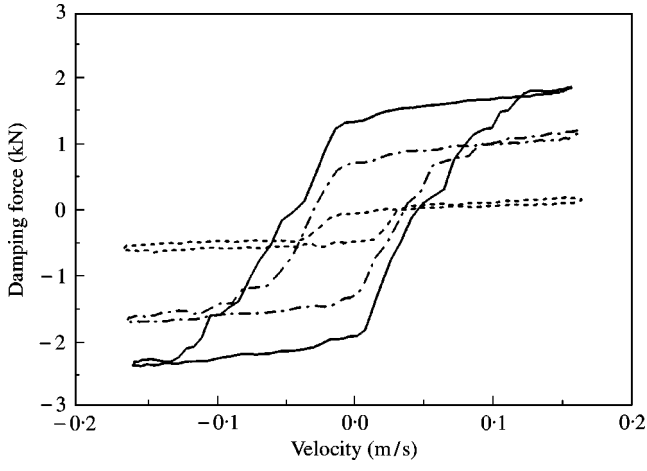

Figure 2. Measured damping force characteristics. -------, 0·0 A; –·–·–·, 1·2 A; ——, 2·0 A.

obtained [1] by

$$F = k_e x_p + c_e v + \alpha_1 \alpha H^{\beta} \operatorname{sign}(v). \tag{2}$$

In the above equation, x_p is the piston displacement, v the piston velocity, k_e the stiffness constant due to the gas compliance, c_e the damping constant due to the viscosity of the MR fluid, and α_1 the geometrical constant. The third term is, of course, the controllable damping force by the input magnetic field (or current) of H.

Figure 3(b) presents a basic mechanism of Bouc–Wen model which is frequently adopted in the analysis of non-linear hysteresis behavior. The damping force of the MR can be given [3] by

$$F = c_0 v + k_0(x - x_0) + \gamma z, \tag{3}$$

where x_0 is the initial displacement due to the gas, γ the pressure drop due to the MR effect (yield stress), and z is obtained by

$$\dot{z} = -\varepsilon |v| z |z|^{n-1} - \delta v |z|^n + Av. \tag{4}$$

In the above, ε, δ and A are experimental parameters of Bouc–Wen model which affect the hysteresis behavior in the preyield region. It is noted that experimental parameters of ε, δ and A are varied with respect to the intensity of the input field. Therefore, it is very difficult to realize an open-loop control system to obtain a desirable damping force.

The schematic configuration of the third model proposed in this work is shown in Figure 3(c). We can divide the hysteresis loop shown in Figure 2 into two regions: positive acceleration (lower loop) and negative acceleration (upper loop). Then, the lower loop or the upper loop can be fitted by the polynomial with the power of piston velocity. Therefore, the damping force of the MR damper can be expressed by

$$F = \sum_{i=0}^{n} a_i v^i, \quad n = 6, \tag{5}$$

where a_i is the experimental coefficient to be determined from the curve fitting. It is noted that in this work the order of the polynomial for the damping force model was chosen on the basis of trial and error. It turned out that the polynomials up to fifth order could not

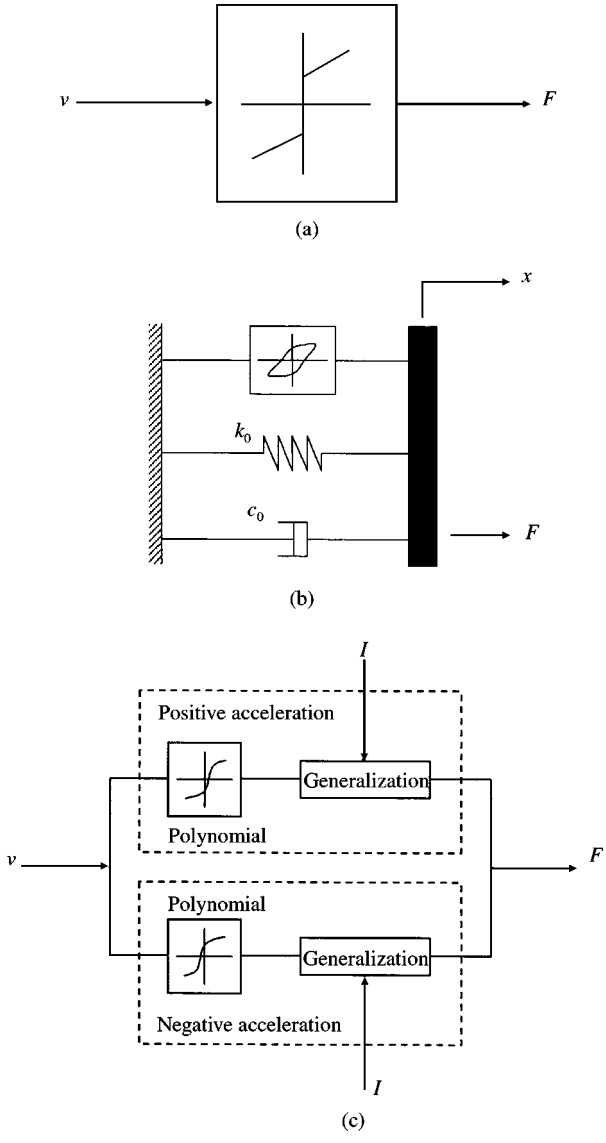

Figure 3. Models for damping force prediction. (a) Bingham model. (b) Bouc-Wen model. (c) Proposed polynomial model.

capture the measured hysteresis behavior. In addition, it has been observed that 6th and higher order polynomials favorably capture the hysteresis behavior without much difference. Therefore, in this work a sixth order polynomial was chosen by considering computational time which is also very important factor in the real-time control of the damping force. The coefficient a_i in equation (5) can be represented with respect to the intensity of the input current as shown in Figure 4. In the plots, the dark square indicates the measured value, and the solid curve is the linear fit of the coefficient a_i. The plots for a_1, a_3, a_4, a_5 and a_6 are referred to in reference [7]. It is clearly observed that the coefficient a_i can be linearized with respect to the input current as follows.

$$a_i = b_i + c_i I, \quad i = 0, 1, \ldots, 6. \tag{6}$$

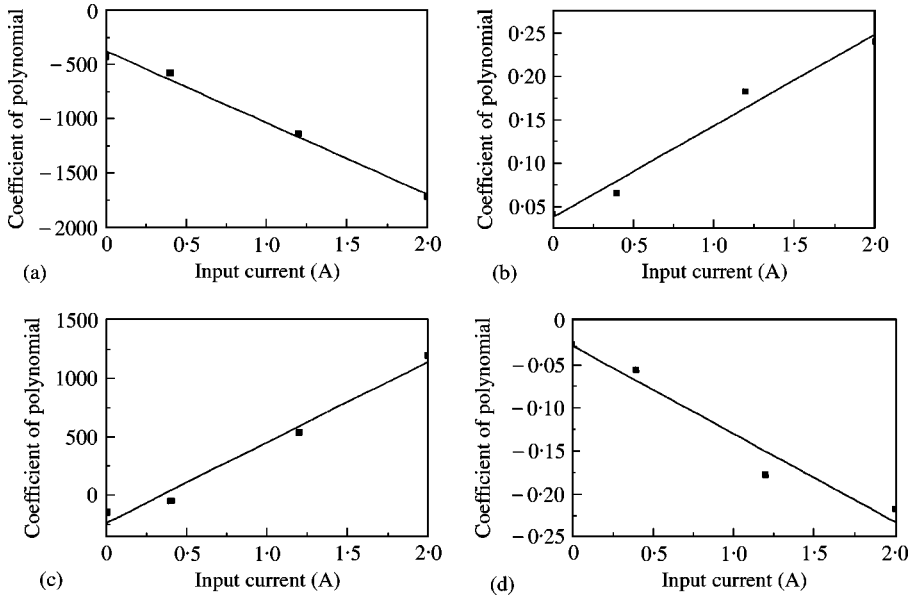

Figure 4. The relationship between a_i and current: as (a) positive acceleration (a_0); (b) positive acceleration (a_2); (c) negative acceleration (a_0); (d) negative acceleration (a_2): ■, a_0 or a_2; ——, linear fit.

TABLE 1

Coefficients b_i and c_i of the polynomial model

Positive acceleration				Negative acceleration			
Parameter	Value	Parameter	Value	Parameter	Value	Parameter	Value
b_0	− 371·8	c_0	− 659·4	b_0	− 235·8	c_0	693·7
b_1	6·205	c_1	8·955	b_1	5·391	c_1	7·034
b_2	0·03728	c_2	0·1062	b_2	− 0·02774	c_2	− 0·1020
b_3	− 3·487e-4	c_3	− 1·584e-4	b_3	− 3·788e-4	c_3	6·729e-5
b_4	− 2·767e-6	c_4	− 5·908e-6	b_4	2·449e-4	c_4	4·967e-6
b_5	6·924e-9	c_5	1·137e-9	b_5	8·804e-9	c_5	− 4·924e-9
b_6	5.604e-11	c_6	1·087e-10	b_6	− 5·374e-11	c_6	− 8·196e-11

As a result, the damping force can be expressed by

$$F = \sum_{i=0}^{n} (b_i + c_i I) v^i. \tag{7}$$

The coefficients b_i and c_i are obtained from the intercept and the slope of the plots shown in Figure 4. The specific values of b_i and c_i used in this work are listed in Table 1. It is noted that the coefficients a_i, b_i and c_i are not sensitive to the magnitude of the input current [7]. Thus, we can easily realize an open-loop control system to achieve a desirable damping force. This is presented in a subsequent section.

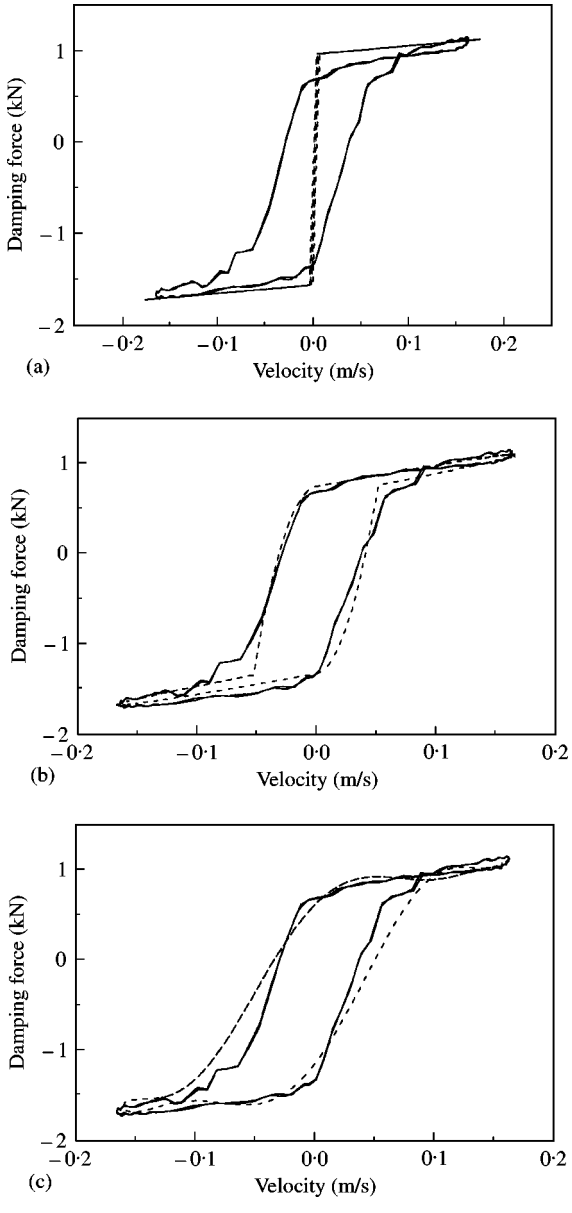

Figure 5. Comparison of damping forces between the measurement and the prediction. (a) Bingham model. (b) Bouc-Wen model. (c) Proposed polynomial model: ——, measured; - - - - - - -, simulated.

3. RESULTS AND DISCUSSION

The measured damping force is compared with the predicted damping forces obtained from the Bingham model, Bouc-Wen model and the proposed polynomial model as shown in Figure 5. The excitation frequency and magnitude are chosen as 1·4 Hz and ± 20 mm respectively. The input current applied to the MR damper is set as 1·2 A. It is clearly observed that the Bingham model cannot capture the non-linear hysteresis behavior, although it fairly predicts only the magnitude of the damping force at a certain piston velocity. On the other hand, the measured hysteresis behavior is well predicted by the

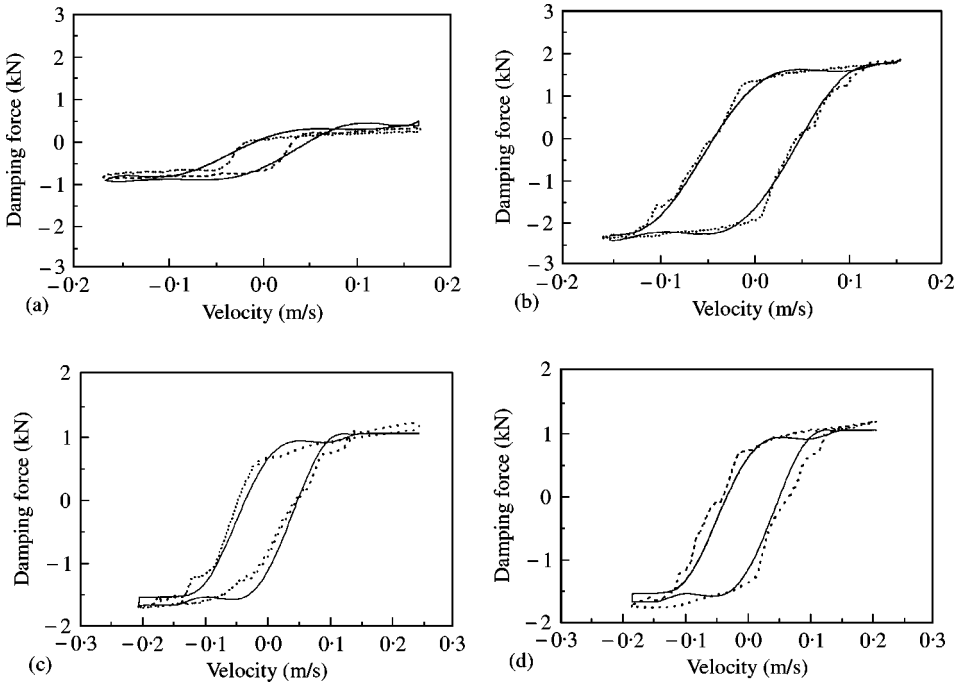

Figure 6. Damping force characteristics at various operating conditions: (a) amplitude: ±20 mm, frequency: 1·4 Hz, input current: 0·4 A; (b) amplitude: ±20 mm, frequency: 1·4 Hz, input current: 2·0 A; (c) amplitude: ±20 mm, frequency: 2·2 Hz, input current: 1·2 A; (d) amplitude: ±25 mm, frequency: 1·4 Hz, input current: 1·2 A: ------, measured; ——, simulated.

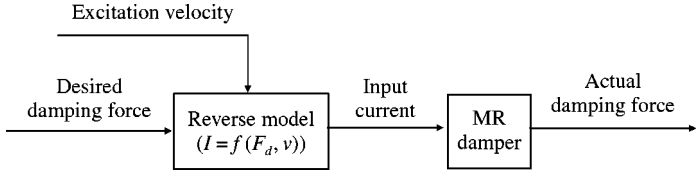

Figure 7. Block-diagram for damping force control.

Bouc-Wen model or the proposed polynomial model. In order to demonstrate the general effectiveness of the proposed model, we change the excitation conditions and the input current. The comparative results between the measurement and the simulation under various operating conditions are shown in Figure 6. We clearly see that the proposed model predicts fairly well the hysteresis behavior under various conditions without modifying the experimental coefficients of a_i, b_i and c_i.

As mentioned earlier, an accuracy of damping force control of the MR damper depends upon the damper model. To demonstrate this, an open-loop control system to achieve a desirable damping force is established as shown in Figure 7. Once the desirable damping force is set in the microprocessor, the control input current to achieve the desirable damping force is determined from the damper model, and applied to the MR damper. For the proposed damper model, the control input is determined from equation (7) and it is given by

$$I = \frac{F_d - \sum_{i=0}^{n} b_i v^i}{\sum_{i=0}^{n} c_i v^i}, \tag{8}$$

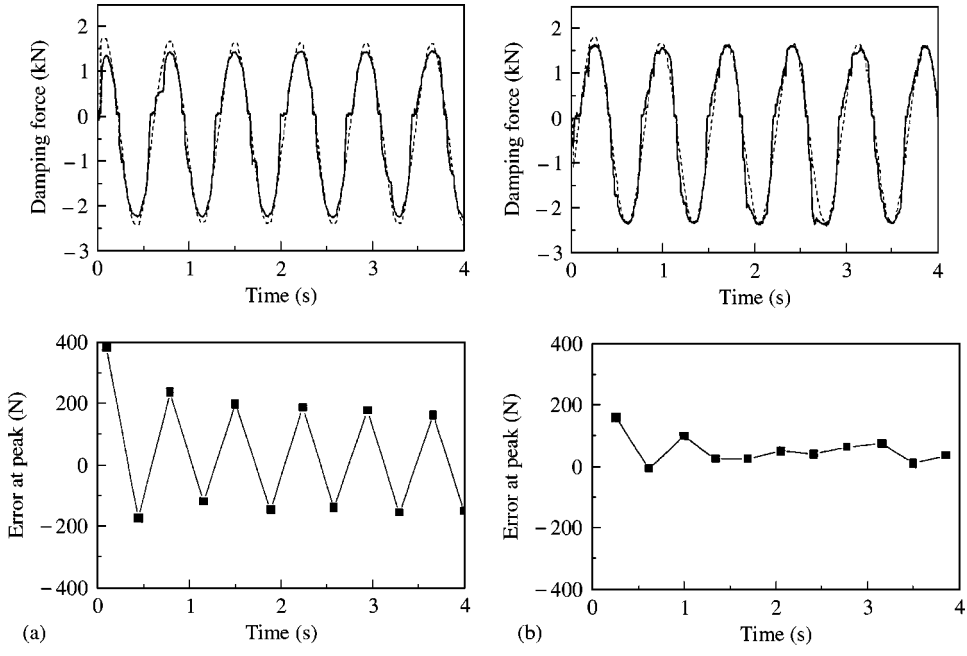

Figure 8. Tracking control responses of the damping force. (a) Bingham model. (b) Polynomial model: ——, measured; - - - - - -; desired.

where F_d is the desirable damping force to be tracked. The desirable damping force is normally set by $F_d = c_{sky}v$. The coefficient c_{sky} is control gain, and it is chosen as 13 000 in this work. Figure 8 presents the damping force controllability realized from the open-loop control system. It is clearly seen that the control accuracy of the proposed model is much better than the Bingham model. In the Bingham model, it is observed that the tracking accuracy at the peak is not so good. This is because the Bingham model cannot capture the damping force behavior at zero and near-zero piston velocity as shown in Figure 5(a). On the contrary, the proposed polynomial model tracks well the desired one in the whole range of the piston velocity.

4. CONCLUDING REMARKS

A hysteresis model for the field-dependent damping force of the MR damper was proposed. The measured damping force is compared with the predicted ones from the Bingham model, Bouc-Wen model, and the proposed polynomial model. It has been demonstrated that the proposed polynomial model predicts fairly well the non-linear hysteresis behavior of the MR damper. The effectiveness of the proposed model was also shown by comparing the measured result with the predicted results at various operating conditions. In addition, the superior control accuracy of the proposed model to the Bingham model was verified by realizing the open-loop control system to track a desirable damping force. It is finally noted that the study showing how much the proposed damper model affects the vibration control performance of ER or MR suspension system needs to be undertaken as a further research.

ACKNOWLEDGMENTS

This work was partially supported by the Korea Science and Engineering Foundation (KOSEF) through the CISD at Yonsei University. This financial support is gratefully acknowledged.

REFERENCES

1. S. B. CHOI, Y. T. CHOI and D. W. PARK 2000 *Journal of Dynamic Systems, Measurement and Control* **122**, 114. A sliding mode control of a full-car ER suspension via hardware-in the-loop-simulation.
2. J. D. CARLSON and J. L. SPROSTON 2000 *Actuator* 2000, *Seventh International Conference on New Actuators*, **126**. Controllable fluid in 2000—status of ER and MR fluid technology.
3. B. F. SPENCER JR., S. J. DYKE, M. K. SAIN and J. D. CARLSON 1997 *Journal of Engineering Mechanics, American Society of Civil Engineers* **123**, 230. Phenomenological model for a magnetorheological damper.
4. N. M. WERELEY, L. PANG and G. M. KAMATH 1998 *Journal of Intelligent Material Systems and Structures* **9**, 642. Idealized hysteresis modeling of electrorheological and magnetorheological dampers.
5. N. D. SIMS, D. J. PEEL, R. STANWAY, A. R. JOHNSON and W. A. BULLOUGH 2000 *Journal of Sound and Vibration* **229**, 207. The electrorheological long-stroke damper: a new modeling technique with experimental validation.
6. S. B. CHOI, Y. T. CHOI, E. G. CHANG, S. J. HAN and C. S. KIM 1998 *Mechatronics* **8**, 143. Control characteristics of a continuously variable ER damper.
7. S. K. LEE 2000 *M.S. Thesis, Inha University, Korea*. Hysteresis model of damping forces of MR damper for a passenger car.